ICRA2026 Late Breaking Results Poster presented at
2026 IEEE International Conference on Robotics and Automation (ICRA 2026)
June 1-5, 2026. Vienna, Austria

Development of a Variable Stiffness High Resolution Tension Sensor for Tendon-Driven Robot Hands

[1]Ginwoo Pyo, [1]Chunghyeon Lee, and [1,†]Seokhwan Jeong
[1]*Department of Mechanical Engineering Sogang University* Seoul, South Korea
[†]Corresponding author: seokhwan@sogang.ac.kr

***Abstract*—Tendon-driven robotic hands face a fundamental *"Triple Trade-Off"* among high force control bandwidth, low mechanical impedance, and precise force estimation. This extended abstract presents a novel variable-stiffness tension sensor designed to overcome these conflicting requirements. By integrating a nonlinear spring mechanism into the tendon routing path, the sensor dynamically modulates its physical stiffness according to the applied tension while simultaneously providing high-resolution force feedback. Experimental results confirm that the system's force control bandwidth dynamically increases from 12.70 Hz to 19.53 Hz as the tendon tension scales up. Furthermore, the feasibility of the system was validated on a 3-DoF tendon-driven robotic finger, successfully demonstrating the sensor's high sensitivity by delicately actuating a 50 gf mechanical keyboard switch at low tensions.**

***Index Terms*—Mechanism Design, Tendon/Wire Mechanism, Compliant Joints and Mechanisms**

I. Introduction

With the rapid advancement of reinforcement learning and AI-based control for robots, there is an increasing demand for hardware capable of human-level dynamic characteristics. In achieving this, the physical design of robotic hands remains a critical bottleneck for complex grasping and object manipulation [1]. The performance of a robotic hand in such dynamic tasks is inherently governed by a "Triple Trade-Off": the difficult balance among high force/torque control bandwidth, low mechanical impedance, and high-resolution force estimation.

Conventional robot hands relying on built-in, high-gear-ratio actuators heavily compromise this trade-off; while providing high positional accuracy and output torque [2], they suffer from low force control bandwidth, high mechanical impedance, and vulnerability to external impacts. Conversely, tendon-based direct-drive structures effectively lower system inertia and mechanical impedance [3] but critically struggle to achieve the high-resolution force estimation required to overcome the triple trade-off, often due to complex friction and hysteresis along the tendon routing [4], [5].

To address these conflicting requirements, we propose a variable-stiffness tension sensor, as shown in Fig. 1. Drawing inspiration from the advantages of variable impedance actuation [6], this sensor is designed for integration into the tendon routing path without compromising the system's mechanical transparency. At low tensions, the sensor exhibits low stiffness, providing the high compliance and low mechanical impedance required for delicate, contact-rich manipulation. At high tensions, it naturally transitions to high stiffness, ensuring rigid force transmission and high bandwidth for heavy load tasks.

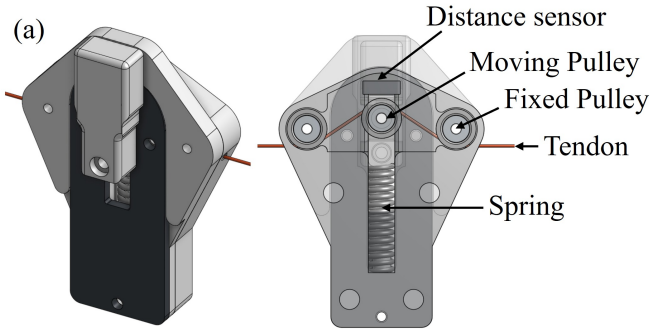

Fig. 1. CAD model of the tension sensor.

The sensor's behavior was mathematically modeled and empirically validated, confirming a nonlinear increase in physical stiffness as a function of tension. The system's dynamic performance was evaluated by measuring the force control bandwidth. Furthermore, implementation on a 3-DoF robotic finger demonstrated force sensitivity and transparency, confirming the system's ability to effectively mitigate the "Triple Trade-Off" problem.

II. Theoretical Modeling

The core mechanism of the proposed sensor translates linear spring compression into a nonlinear tension profile, establishing a variable stiffness transmission. By mathematically modeling the tendon routing kinematics and the pulley displacement, the tendon tension can be explicitly derived. The governing tension equation is defined as a function of θ:

$$T(\theta) = \frac{K(y_0 - y(\theta))}{2\sin\theta} \tag{1}$$

where K is the spring constant of the internal spring, y_0 is the default height of the moving pulley, $y(\theta)$ is the pulley height

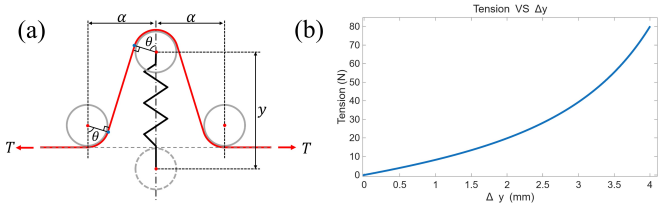

Fig. 2. (a) Diagram of the nonlinear spring mechanism. (b) Graph showing the nonlinear relationship of the pulley displacement vs tension.

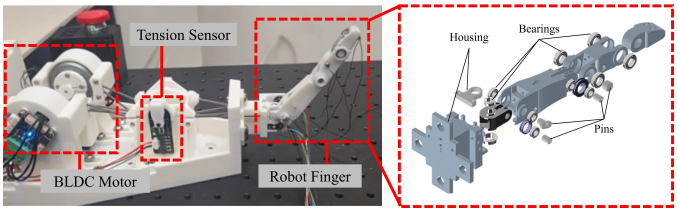

Fig. 3. Experimental setup of the single-finger test platform, showing the proposed tension sensor integrated into the tendon transmission path.

at the current state, and θ is the tendon routing angle as shown in Fig. 2(a). The displacement $y(\theta)$ can also be modeled as a function of θ:

$$y(\theta) = \tan\theta(\alpha - 2r\sin\theta) - 2r(\cos\theta - 1) \qquad (2)$$

This formulation establishes a direct framework for precisely estimating tension from small displacements, while the apparent stiffness of the system varies nonlinearly with respect to the applied load as shown in Fig. 2(b).

III. Hardware Design

The sensor housing was manufactured primarily via fused deposition modeling (FDM) 3D printing using PLA filament, with a linear spring with a stiffness of 9.8 N/mm. To achieve high-resolution displacement measurement, a TCRT 1000 (Vishay®) optical distance sensor was selected. The design variables α and y_0 were specifically chosen so that the center moving pulley displacement is restricted to 4 mm under an 80 N tension load. This range was optimized because the TCRT 1000 sensor exhibits peak displacement sensitivity at target distances between 1–5 mm. A custom PCB was developed to mount the sensor and simultaneously act as an integrated part of the structural housing.

To ensure signal integrity and mitigate high-frequency noise or aliasing, the PCB features a dedicated analog low-pass filter and a ferrite bead. Furthermore, digital signal interference is inherently blocked by isolating the dedicated analog power (VDDA) and analog ground (VSSA). For system validation, the variable-stiffness sensor was integrated into a 3-DoF, antagonistically routed, tendon-driven robot finger, as shown in Fig. 3.

IV. Experiments and Results

Experimental frequency response analysis demonstrated the variable stiffness capability; as the applied tension scaled up from 23.3 N to 56.7 N, the measured force control bandwidth (-3 dB cutoff frequency) dynamically increased from 12.70 Hz to 19.53 Hz. To validate mechanical transparency and sensitivity, the sensor-equipped finger was tested by pressing a 50 gf mechanical keyboard switch, as shown in Fig. 4. These results demonstrate that the proposed system maintains the delicate sensitivity required for light interactions while having the capacity to rigidify for high-bandwidth tasks.

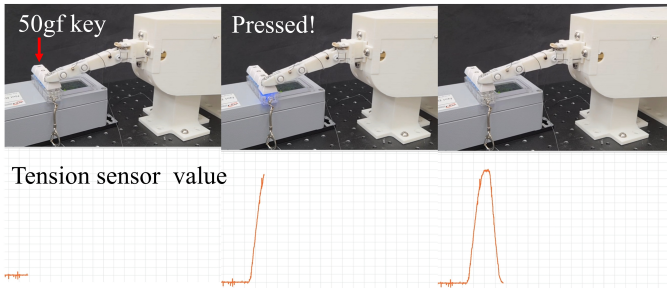

Fig. 4. Experimental validation of the robotic finger pressing a 50 gf mechanical keyboard switch. The bottom plot illustrates the estimated tension, demonstrating the high force sensitivity of the proposed sensor.

V. Conclusion and Future Work

This work introduces a nonlinear spring-based tension sensor that mitigates the triple trade-off for tendon-driven robotic hands. By merging a variable stiffness mechanism with precise optical displacement sensing, the system achieves both compliant interaction and robust force transmission. Future work will focus on developing a fully functional five-fingered robot hand equipped with the proposed tension sensor.

Acknowledgment

This work was supported by the National Research Foundation of Korea (NRF) grant funded by the Korea government (MSIT) (RS-2025-16070605) and the Nano Material Technology Development Program through the NRF funded by the Ministry of Science and ICT (RS-2025-25442536).

References

[1] U. Kim, D. Jung, H. Jeong, J. Park, H.-M. Jung, J. Cheong, H. R. Choi, H. Do, and C. Park, "Integrated linkage-driven dexterous anthropomorphic robotic hand," *Nature Communications*, vol. 12, no. 1, p. 7177, Dec. 2021.

[2] R. Ozawa, H. Kobayashi, and K. Hashirii, "Analysis, Classification, and Design of Tendon-Driven Mechanisms," *IEEE Transactions on Robotics*, vol. 30, no. 2, pp. 396–410, Apr. 2014.

[3] Y. Wang, W. Li, S. Togo, H. Yokoi, and Y. Jiang, "Survey on Main Drive Methods Used in Humanoid Robotic Upper Limbs," *Cyborg and Bionic Systems*, vol. 2021, Jun. 2021.

[4] G. Palli, G. Borghesan, and C. Melchiorri, "Modeling, Identification, and Control of Tendon-Based Actuation Systems," *IEEE Transactions on Robotics*, vol. 28, no. 2, pp. 277–290, Apr. 2012.

[5] L. Chen, X. Wang, and W. L. Xu, "Inverse Transmission Model and Compensation Control of a Single-Tendon–Sheath Actuator," *IEEE Transactions on Industrial Electronics*, vol. 61, no. 3, pp. 1424–1433, Mar. 2014.

[6] B. Vanderborght, A. Albu-Schaeffer, A. Bicchi, E. Burdet, D. G. Caldwell, R. Carloni, M. Catalano, O. Eiberger, W. Friedl, G. Ganesh, M. Garabini, M. Grebenstein, G. Grioli, S. Haddadin, H. Hoppner, A. Jafari, M. Laffranchi, D. Lefeber, F. Petit, S. Stramigioli, N. Tsagarakis, M. Van Damme, R. Van Ham, L. C. Visser, and S. Wolf, "Variable impedance actuators: A review," *Robotics and Autonomous Systems*, vol. 61, no. 12, pp. 1601–1614, Dec. 2013.